optica

Integrated nanophotonic wavelength router based on an intelligent algorithm: supplementary material

ZHOUHUI LIU,[1†] XIAOHONG LIU,[1,2†] ZHIYUAN XIAO,[1†] CUICUI LU,[1,*] HUI-QIN WANG,[2] YOU WU,[3] XIAOYONG HU,[3,5] YONG-CHUN LIU,[4] HONGYU ZHANG,[1] AND XIANGDONG ZHANG[1,6]

[1]*Beijing Key Laboratory of Nanophotonics and Ultrafine Optoelectronic Systems, School of Physics, Beijing Institute of Technology, Beijing 100081, China*

[2] *Physics Department, School of Sciences, Nanchang University, Nanchang 330031, China*

[3]*State Key Laboratory for Mesoscopic Physics & Department of Physics, Collaborative Innovation Center of Quantum Matter, Beijing Academy of Quantum Information Sciences, Nano-optoelectronics Frontier Center of Ministry of Education, Peking University, Beijing 100871, China*

[4]*State Key Laboratory of Low-Dimensional Quantum Physics, Department of Physics, Frontier Science Center for Quantum Information, Collaborative Innovation Center of Quantum Matter, Tsinghua University, Beijing 100084, China*

[5] *e-mail: xiaoyonghu@pku.edu.cn*

[6]*e-mail: zhangxd@bit.edu.cn*
**Corresponding author: cuicuilu@bit.edu.cn*

Published 15 October 2019

This document provides supplementary information to "Integrated nanophotonic wavelength router based on an intelligent algorithm," https://doi.org/10.1364/OPTICA.6.001367.

1. ALGORITHM DETAILS

A. Feature of the Intelligent Algorithm

The intelligent algorithm is implemented primarily with genetic algorithm (GA) and the finite element method (FEM). Above all, the special solving mechanism of genetic algorithm makes it perform well at global optimization [1]. This is because it begins with a string of solutions to a problem, covering a large area, rather than a single solution like some traditional optimization algorithms. In addition, finite element method, which is adopted to calculate the transmission spectrum of the structures, facilitates analyzing such disordered complex structures due to its mesh adaptation method [2]. It provides refined mesh in complex area and regular mesh in simple area, getting more accurate solution and meanwhile saving computing time. Besides, the genetic algorithm does not rely on the gradient of the fitness function, which makes it less likely to fall into local minima compared to other optimization algorithms. In case the result is suspect to be a local minimum, we have several tips to solve this problem. First, we can adjust the mutation rate to be higher, which contribute to create multiple children population to jump out a local minimum. Second, when the result is suspect to be a local minimum, we can input its parameters as one of the initial chromosomes to start a new optimization. Third, we can increase the iterations meaning that they have more chances to create new children populations. Also, we can run the algorithm multiple times with different random initial populations and compare the performance of their results to see how severe this problem is for a particular design. By iterating with GA and FEM method, the algorithm can show the detailed real-time electromagnetic field in any time of the iteration. Besides, due to the special solving mechanism of GA, it may ignore the underling physics, but still succeed in many optic design areas, which may contribute to help researchers discover novel structures and functions without the limit of existing theories [3].

B. Fitness Function

One of the most important parts of the algorithm is the fitness function. It is employed as both a performance evaluation criteria and an objective function that is a special feature of genetic algorithm. Individual's fitness is the value of fitness function, representing the performance of them, which indicates each channel's percentage transmittance. Finding the minimum of this function efficiently and accurately is the intelligent algorithm's task. Signals function and noise function were created to express which bandwidth is wanted and which is unwanted. We used S to indicate signals function, and S_j ($j = 1, 2, 3, \ldots, J$) indicates the central wavelength transmittance to be optimized of the j-th channel. The relationship is defined as:

$$S = J\left(\sum_j \frac{1}{S_j}\right)^{-1} \quad \textbf{(S1)}$$

It is the harmonic mean of signals intensity. During the iteration, the value of S is expected to be increased. The increasing rate of S enormously depends on the variable with smaller value. S has theoretical maximum value ' 1 ' only if S_1, S_2, ..., S_j are equal to 100%. The function gives every channel short odds to be optimized. As for the noise function, root-mean-square error (RMSE) is employed, which is universally applied to describe the dispersion degree of distribution in the fields of statistics. The noise function is expressed as:

$$N=\left(\sum_i \frac{\left(N_i - N_0\right)^2}{i}\right)^{1/2} \quad \textbf{(S2)}$$

where N_i (i = 1, 2, 3, ..., I) presents all the noise energy transmittance, and N_0 indicates the target average noise which is set to be ' 0 '. The method by using RMSE assures that all noise is dramatically close to ' 0 ', and provides a high signal-to-noise ratio. During the iteration, the value of N is expected to be decreased. Because the larger value of noise will enormously influence the whole value of noise function, noise of higher intensity will be firstly decreased. Since the sensitivity of the target to the design parameters is not deterministic in genetic algorithms, it caused challenges in the disordered structure with so many variables. Here, the objective function can balance these variables, by combining signals function and noise function. The final fitness function is defined as:

$$F=\left(\sum_i \frac{\left(N_i - N_0\right)^2}{i}\right)^{1/2} - J\left(\sum_j \frac{1}{S_j}\right)^{-1} \quad \textbf{(S3)}$$

It is the intelligent algorithm's task to find the minimum of this function. When F gets its minimum value, S is maximum and N is the minimum, guaranteeing high enough signal strength and insuring adequately low-level noise. Meanwhile, it provides a strong optimization guidance and speed up the convergence rate of the algorithm.

C. Selection, Mutation and Convergence Condition

Genetic algorithm encodes the population similarly to biological gene coding. The all design parameters such as width, height and position compose a 'chromosome'. In this work, 30 chromosomes were prepared as the first generation. A chromosome corresponds to a device structure and is coded by the algorithm for crossover and mutation. After the binary encoding, each chromosome has the same length. Assume that parent 1 is '10011011' and parent 2 is '01011001'. During crossover, the two parent chromosomes are intermixed, to generate two children populations to replace the parent populations, where the crossover point is randomly picked. If the crossover point is 3, we swap the first 3 code of parent 1 and parent 2, then we got child 1 '01011011' and child 2 '10011001'. A frequently used method, roulette-wheel selection method, is applied to selecting the potential superiority gene. The individuals who behave better are more likely to be reserved. In the design, we set 50% chance for the selected chromosomes to cross with others. In addition, each binary code has 10% mutation probability, which is in favor of the evolution. Then, a new child population is created through the 'chromosome' combination, being the same size with parent population. The convergence condition is that the fitness of the best individual does not reduce by a considerable value for more than 50 generations, or the results has already met the requirements.

2. MORE SIMULATION RESULTS

A. Three-Channel Wavelength Router of Metal/Air Material

A three-channel wavelength router with silver and air as the material is also designed and shown in Fig. S1. (a), which covers 1.1 μm × 1.1 μm. In this structure, 4 × 4 silver rectangles are preset, and the process of optimization can automatically filter out the structural unit which is too small. The refractive index for air is 1.0, and the wavelength-dependent complex refractive index function of silver is taken from Ref. [4]. The objective center wave-length is set to be 450 nm, 600 nm and 800 nm with a near-Gaussian line shape, and other wavelength ranges are inhibited. The calculated transmission spectrum is shown in Fig. S1 (b). When the TM-polarized light with a range of 350 nm to 1100 nm is incident to the left input port, only the center wavelength of 450 nm, 600 nm and 800 nm channels can transmit through the output ports. The corresponding simulated magnitude of the electric field for the three wavelengths are plotted in Fig. S1 (c) (d) and (e). It is very clear that the electromagnetic waves for wavelengths 450 nm, 600 nm and 800 nm propagate into different output ports, respectively. The transmittance of the three channels are 34%, 34% and 53% respectively.

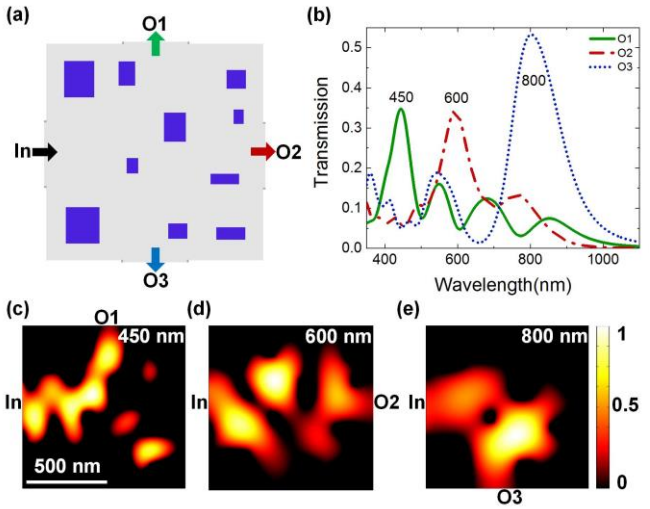

Fig. S1. Three-channel wavelength router for metal materials. (a) Structure of the router. The blue holes are silver and the white area is filled with air. The size of the structure is 1.1 μm × 1.1 μm. (b) Simulated transmission spectrum covers from 350 nm to 1100 nm, where the transmission peaks are λ = 450 nm, λ = 600 nm and λ = 800 nm, respectively. **In** denotes input port, **O1**, **O2** and **O3** are the upper output port, the right output port and the lower output port, respectively. (c) (d) and (e) Simulated magnitude of the electric field for 450 nm, 600 nm and 800 nm, respectively.

B. Two-Channel Wavelength Router of Dielectric Material

We also designed a two-channel wavelength router with different output ports locations by using two materials of silicon and silicon dioxide for integration. The device geometry is shown in Fig. S2 (a). The purple squares denote silicon and the gray area indicates silicon dioxide, where n_{si} = 3.45, and n_{sio2} = 1.45. The designed area is 1.5 μm × 1.5 μm, in which 5 × 5 initial silicon squares are placed and the size of the square is set to be 140 nm × 140 nm. In addition, a 300 nm wide input port (In) is at the center of left boundary, and two output ports are located in the upper right boundary (O1) and

lower right boundary (O2) in the same size, respectively. Actually, either the number or size of the squares or the position and width of the ports can be arbitrarily assigned. Specific wavelength signal being transmitted through the two output ports is expected. Considering the practical communication applications, 1300 nm and 1550 nm are the widely used optical communication range. Therefore, in the design, the objective center wavelength is set to be 1300 nm and 1550 nm with a near-Gaussian line shape. Except the two signals, other wavelength range is regarded as noise to be inhibited. By using the IA, we can determine all the parameters above. The calculated transmission spectrum is shown in Fig. S2 (b). When TM-polarized continuum-wave (CW) light with a range of 1100 nm to 1800 nm was incident to the left input port, only the center wavelength of 1300 nm and 1550 nm can transmit through the output ports, where the full width of the half maximum (FWHM) is 55 nm and 171 nm, respectively. The corresponding simulated power flows on time average of the two wavelengths are plotted in Fig. S2 (c) and (d). It is very clear that the electromagnetic waves of wavelengths 1300 nm and 1550 nm propagate into different output ports, respectively. The transmittance of the two channels are 38% and 29% respectively, and we get low transmission (less than 5%) for all the noise wavelength range, meaning that it successfully filtered the noise we set. The final structure is designed after 200 iterations, in about 3 hours using a personal computer with 4 Intel (R) Core (TM) i7-7500U CPU at 2.7 GHz, and 8 GB installed memory (RAM, random-access memory). It is worth mentioning that the efficiency can be further improved with the increase of iteration times and time extension. The realized wavelength router possesses ultra-small footprint of 1.5 μm × 1.5 μm, and its operation band covers the optical communication range. The developed IA can be used for more cell quantities and different output ports besides upper right and lower right.

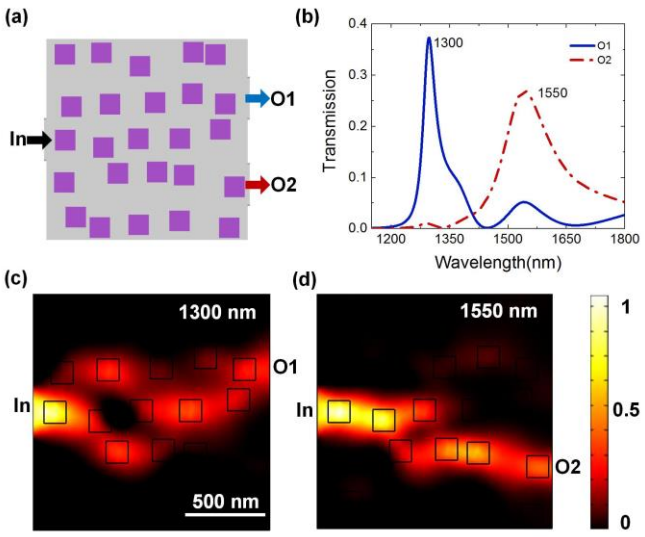

Fig. S2. Two-channel wavelength router for dielectric materials (a) Structure of the router. The size of the structure is 1.5 μm × 1.5 μm. The light gray area indicates silicon dioxide, the purple rectangle denotes silicon. (b) Simulated transmission spectrum covering from 1,100 nm to 1,800 nm. The transmission peaks are λ = 1300 nm and λ = 1550 nm, respectively. **In** is the input port, **O1**, **O2** are the upper right output port and the lower right output port, respectively. (c) (d) Simulated power flow on time average at 1300nm and 1550nm, respectively.

C. Two-Channel Router with More Cells

By increasing the number of square cells to be 8 × 8, a two-channel wavelength router is designed, the design area is 2 μm × 2 μm, and the squares' size is 100 nm × 100 nm. A 500 nm wide input port (In) is on the center left boundary, and two 500 nm wide output ports are in the upper center (O1) and the lower center (O2) of the boundaries, respectively. The device geometry is shown in Fig. S3 (a). The purple rectangle denotes silicon and the gray area indicates silicon dioxide, where n_{si} = 3.45, and n_{sio2} = 1.45. In the design, the objective center wavelengths are set to be 1300 nm and 1550 nm with a near-Gaussian line shape, which are the widely used optical communication range. In addition to the two signal bands, other wavelength ranges are regarded as noise. The calculated transmission spectrum is shown in Fig. S3 (b). When the TM-polarized light with a range of 850 nm to 1500 nm is incident to the left input port, only the center wavelength of 1050 nm and 1300 nm channels can transmit through the output ports, where the full width of the half maximum (FWHM) is 104 nm and 149 nm, respectively. The corresponding simulated power flow on time average of the two wavelengths are plotted in Fig. S3 (c) and (d). It is very clear that the electromagnetic waves for wavelengths 1300 nm and 1550 nm propagate into different output ports, respectively. The transmittance of the two channels are both 40%, and we get low transmission (less than 5%) for all the noise wavelength range.

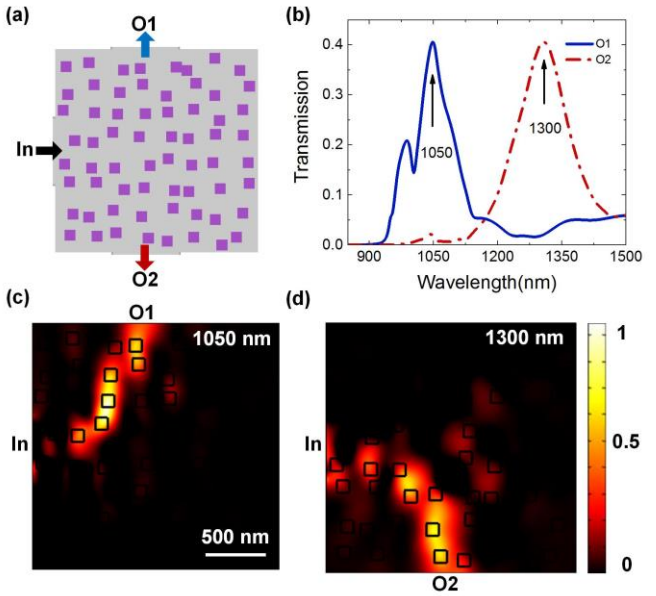

Fig. S3. Two-channel wavelength router. (a) Structure of the router. The light gray area indicates silicon dioxide, the purple squares denote silicon. The size of the structure is 2 μm × 2 μm. (b) Simulated transmission spectrum covering from 850 nm to 1500 nm, where the peaks corresponding to the wavelength of 1050 nm and 1300 nm. **In** denotes input port, **O1**, **O2** are the upper output port and the lower output port. (c) (d) Simulated power flow on time average at 1050 nm and 1300 nm, respectively.

D. Three-Channel Router in Longer Wavelength Range

By changing the three objective center wavelengths to 1050nm, 1300 nm, and 1550nm, we designed a three-channel wavelength router in longer wavelength range. The structure of the router in optical communication wavelength range is showed in Fig. S4 (a). The design region occupies a 2 μm × 2 μm footprint. 5 × 5 silicon squares are put on the silicon dioxide substrate, where n_{Si} = 3.45, and n_{SiO2} = 1.45. The consistent size of square is set to be 140nm × 140 nm. A 500 nm wide input port (In) is on the center of left boundary, and three output ports are in the upper center (O1), the lower center (O2) and the righter center (O3) of the boundaries in the same size, respectively. The calculated transmission spectrum is

shown in Fig. S4 (b). When the TM-polarized light with a range of 900 to 1700 nm is incident to the left input port, only the center wavelength of 1050nm, 1300 nm and 1550nm channels transmit through the output ports, where the FWHM are 96 nm, 67 nm, and 118 nm, respectively. The transmittance of the three channels are 37%, 43% and 39%, respectively, and we got very low crosstalk. The corresponding simulated power flow on time average, y and -y component of the two wavelengths are plotted in Fig. S4 (c), (d) and (e). It is very clear that the electromagnetic waves for wavelengths 1050 nm, 1300 nm and 1550 nm propagate into different output ports, respectively.

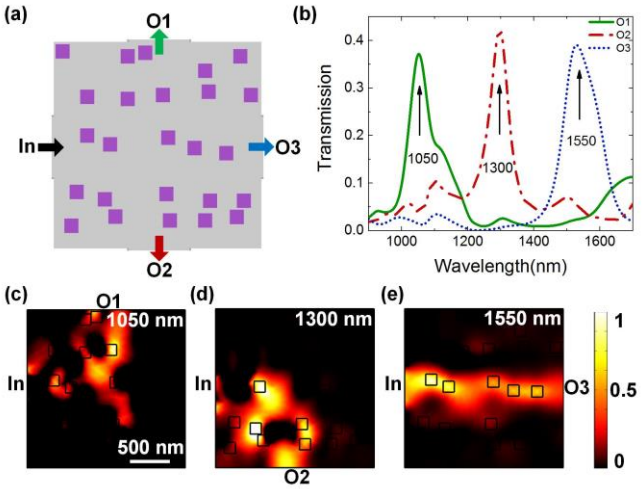

Fig. S4. Three-channel wavelength router in communication wavelength range. (a) Structure of the router. The light gray area indicates silicon dioxide, the purple squares denote silicon. The size of the structure is 2 μm × 2 μm. (b) Simulated transmission spectrum covering from 900 nm to 1700 nm, where the peaks corresponding to the wavelength of 1050 nm, 1300 nm and 1550 nm. **In** denotes input port, **O1**, **O2** and **O3** are the upper output port, the lower output port and the right output port. (c) (d) and (e) Simulated power flow on time average, at 1050 nm, 1300 nm and 1550 nm, respectively.

E. Three-Channel Router with Triangle-Shaped Cell Structures

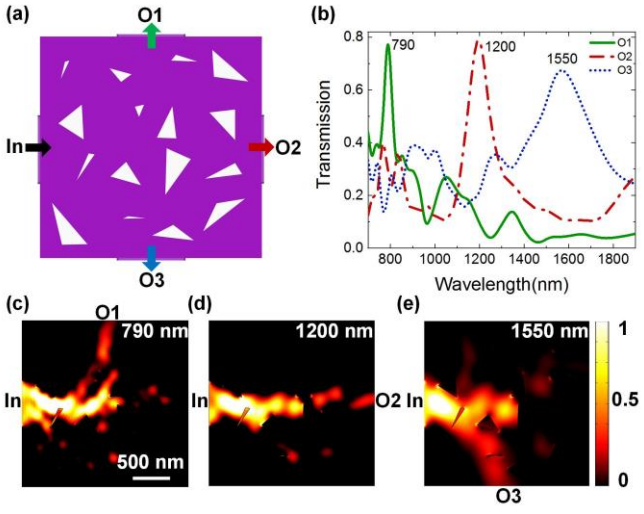

Fig. S5. Wavelength router with triangle air holes. (a) Structure of the router. The white holes represent air and the purple area is silicon. The size of the structure is 1.9 μm × 1.9 μm. (b) Simulated transmission spectrum covering from 700 nm to 1900 nm. The wavelength 790 nm, 1200 nm and 1550 nm are separated to the upper port, right port and lower port respectively. **In** denotes input port, **O1**, **O2** and **O3** are the upper output port, the right output port, and the lower output port. (c) (d) and (e) Simulated energy density on time average of the three wavelengths.

By changing the shape of cell structures, a three-channel router with triangle shaped holes is designed, shown in Fig. S5. (a). The size of the router is 1.9 μm ×1.9 μm, in which 4 × 4 initial air holes are put in the silicon, where refractive index of n_{Si} = 3.45, and n_{air} = 1 are used. In the design, the object center wavelength is set to be 790 nm, 1200 nm and 1550 nm with a near-Gaussian line shape, and other wavelength range is regarded as noise as before. The positions of three vertexes of each triangle are set as variables. Then, we determine all the variables using the IA. The calculated transmission spectrum is shown in Fig. S5 (b). When TE-polarized light with a range of 700 nm to 1900 nm is incident to the left input port, only the center wavelength of 790 nm, 1200 nm and 1550 nm channels can transmit through the output ports. The corresponding simulated energy density on time average of the three wavelengths is plotted in Fig. S5 (c), (d) and (e), respectively. It is very clear that the electromagnetic waves for wavelengths 790 nm, 1200 nm and 1550 nm propagate into different output ports, respectively. The transmittance of the three channels is 77%, 79% and 67% respectively. Like the first model of two-channel wavelength router, more than one output port could be set on one boundary of the router chip. Follow this idea, the realization of more-channel router is possible. From the simulation results above, it presents innovation and multiple design schemes by determining the parameters, and therefore the IA is a method for universal design of the nanophotonic wavelength routers.

F. Three-Channel Router with Circle-Shaped Cell Structures

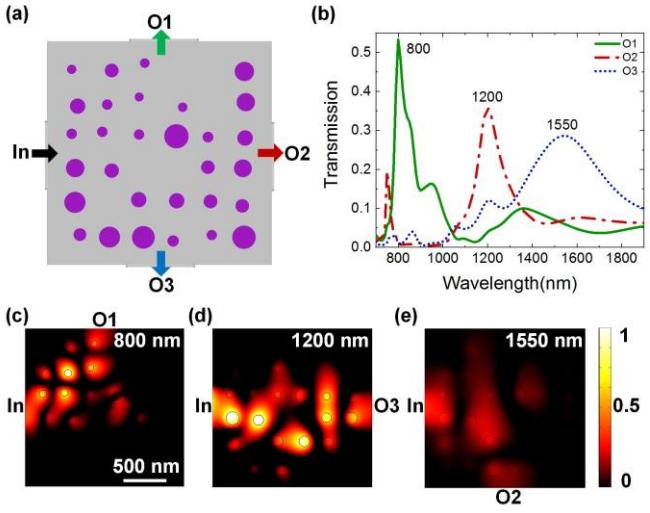

Fig. S6. Three-channel wavelength router with circle air holes. (a) Structure of the router. The purple holes are silicon, while the remaining gray area is filled with silicon dioxide. The size of the structure is 1.5 μm × 1.5 μm. (b) Simulated transmission spectrum covered from 650 nm to 1950 nm, where the transmission peaks are λ = 800 nm, λ = 1200 nm and λ = 1550 nm, respectively. **In** denotes input port, **O1**, **O2** and **O3** are the upper output port, the right output port and the lower output port, respectively. (c) (d) and (e) S magnitude of the electric field for 800 nm, 1200 nm and 1550 nm. It is very clear that the electromagnetic waves for wavelengths 800 nm, 1200 nm and 1550 nm propagate into different output ports, respectively.

By changing the shape of holes, a router with circle shaped holes is also designed and shown in Fig. S6. (a), which covers 1.5 μm ×1.5 μm. In this structure, 6 × 6 silicon circles are put on the SiO_2 substrate, and the process of optimization can automatically filter out the structural unit which is too small. The refractive of n_{Si} = 3.45, and n_{SiO2} = 1.45 are used. The object center wave-length is set to be 800 nm, 1200 nm and 1550 nm with a near-Gaussian line shape, and other wavelength ranges are inhibited. The position of center and the radius of each circle are set as parameters, which then determined by the algorithm. The calculated transmission spectrum is shown in Fig. S6 (b). When the TM-polarized light with a range of 650 nm to 1950 nm is incident to the left input port, only the center wavelength of 800 nm, 1200 nm and 1550 nm channels can transmit through the output ports. The corresponding simulated energy densities on time average of the three wavelengths are plotted in Fig. S6 (c) (d) and (e). The transmittance of the three channels are 53%, 36% and 29% respectively, and we obtain low crosstalk.

Compared with the results with other shaped holes, the transmission is relatively lower for routes with circle shapes, because the reflection of the square and triangle shape have better directions, the energy flow can be focused better.

G. The Position Error Tolerance of the Devices

In order to illustrate the position error tolerance of our devices, which is defined as the maximum distance shift for each cell, we vary the positions to analyze the influences on device performance. It is acceptable for the devices only if the center wavelength shifts do not exceed 50 nm (about 3% for the infra-red light and 6% for the shorter wavelength of designed routers), the maximum transmissions of the channels decrease no more than 0.1, and the absolute increase of the maximum value of noise for each wavelength does not exceed 0.1. We simulate all the router models under such standards and repeat 20 times randomly for each error tolerance to ensure the reliability.

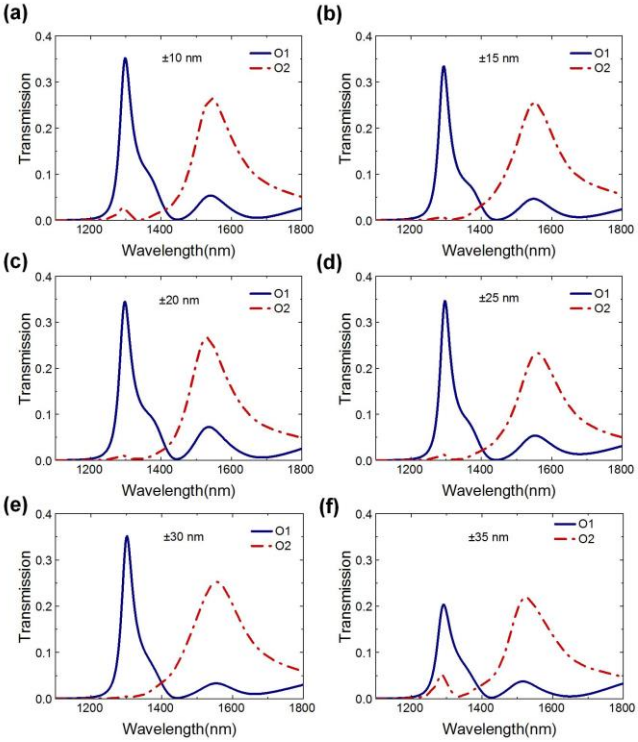

Fig. S7. (a-f) The transmission spectrums of models with cell structure position errors of ±10 nm, ±15 nm. ±20 nm, ±25 nm, ±30 nm and ±35nm, respectively.

Take the model of two-channel router for example (mentioned in section 2 B). Here we show the results of ±10 nm, ±15 nm. ±20 nm, ±25 nm, ±30 nm and ±35nm in Fig. S7 (a-f) respectively. It is clear that the transmission performances of the operating wavelengths (1300 nm and 1550 nm) keep high similarity to the original model that shown in Fig. S2 (b) when the position error doesn't exceed ±30 nm Fig. S7 (a-e). The intensity of signals only decreases 3% (from 38% to 35%), and the intensity of noise still keeps low level, less than 3%, shown in Fig. S7 (e) However, when the the position error is up to ±35 nm, whose transmission spectrum is shown in Fig. S7 (f), it performs low transmissions for the two channels, only 20%. Above all, we consider that the position error tolerance for each cell structure is ±30 nm for this wavelength routers. The other models are test in the same method and under the same standards.

3. 3D CALCULATION AND EXPERIMENT

A. Effective 2D Model and 3D Model

It is very time-consuming to directly optimize 3D model. After investigation and comparison, we found a way to use 2D model in place of 3D model by using the effective refractive index. It turns out that our method is a good match between 2D and 3D. As shown in Fig. S8 (a) it is one of the structures which are optimized by intelligent algorithm. The refractive index of little purple rectangles is 2.8 and the material of the gray area is air whose refractive index is 1.0. The transmission spectrum corresponding to this structure is shown in Fig. S8 (b). Then we built a 3D model based on Fig. S8 (a), as shown in Fig. S8 (c) and the transmission spectrum of 3D structure is shown in Fig. S8 (d). It is observed that the lineaments and center wavelengths for each port of 3D and 2D transmission spectra are almost identical. The method can help us greatly save the 3D calculation time. As for the transmittance, the 2D model is infinitely long in the z-direction, which doesn't form localized modes and guide modes in z-direction. But the thickness is limited in the 3D model and the substrate is silicon dioxide, so the 3D model exists the location in the z-direction, and correspondingly its transmittance is higher than that of 2D model.

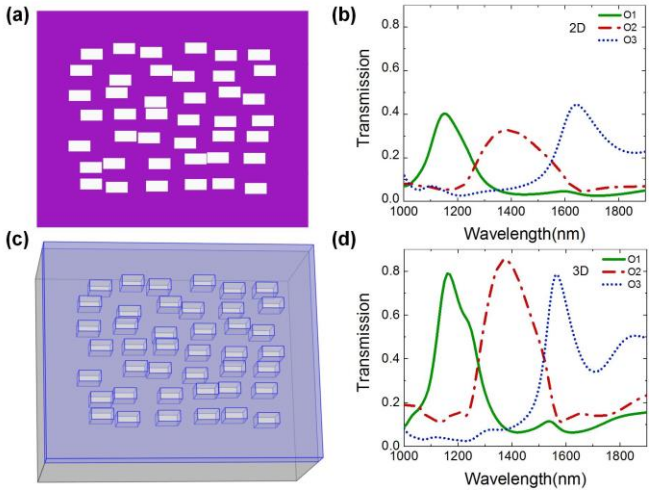

Fig. S8. (a) Structure of the 2D wavelength router. (b) Simulated transmission spectrum of 2D structure. (c) The 3D structure corresponding to Fig. S7 (a). (d) Simulated transmission spectrum of the 3D structure.

[†]These authors contributed equally to this work.

REFERENCES

1. M. Minkov and V. Savona, “Automated optimization of photonic crystal slab cavities,” Sci. Rep. 4, 5124 (2014).
2. COMSOL, Inc., COMSOL Multiphysics Reference Manual, version 5.3, “www.comsol.com," (2018).
3. A. Y. Piggott, J. Lu, T. M. Babinec, K. Petykiewicz, and J. Vuckovic, "Inverse design and implementation of a wavelength demultiplexing grating coupler," Sci. Rep. 4, 7210 (2014).
4. P. B. Johnson and R. W. Christy, "Optical constants of the noble metals," Phys. Rev. B 6, 4370-4379 (1972).